Research article

A motion control method for omni-directional mobile robots based on anisotropy

Chuntao Leng
School of Mechanical Engineering, Shanghai JiaoTong University, Shanghai, China, and

Qixin Cao and Charles Lo
Research Institute of Robotics, Shanghai JiaoTong University, Shanghai, China

Abstract

Purpose – The purpose of this paper is to propose a suitable motion control method for omni-directional mobile robots (OMRs) based on anisotropy.

Design/methodology/approach – A dynamic modeling method for OMRs based on the theory of vehicle dynamics is proposed. By analyzing the driving torque acting on each axis while the robot moves in different directions, the dynamic anisotropy of OMRs is analyzed. The characteristics of dynamic anisotropies and kinematic anisotropies are introduced into the fuzzy sliding mode control (FSMC) system to coordinate the driving torque as a factor of influence.

Findings – A combination of the anisotropy and FSMC method produces coordinated motion for the multi-axis system of OMRs, especially in the initial process of motion. The proposed control system is insensitive to parametric vibrations and external disturbances, and the chattering is apparently decreased. Simulations and experiments have proven that an effective motion tracking can be achieved by using the proposed motion control method.

Research limitations/implications – In order to obtain a clearer analysis of the anisotropy influence during the acceleration process, only the case of translation motion is discussed here. Future work could be done on cases where there are both translation and rotation motions.

Practical implications – The proposed motion control method is applied successfully to achieve effective motion control for OMRs, which is suitable for any kind of OMR.

Originality/value – The novel concept of dynamic anisotropy of OMRs is proposed. By introducing the anisotropy as an influential factor into the FSMC system, a new motion control method suitable for OMRs is proposed.

Keywords Robotics, Control technology, Torque

Paper type Research paper

1. Introduction

Different from traditional mobile robots, omni-directional mobile robots (OMRs) can achieve translation along any arbitrary direction without rotation, which results in their agile performance (Pin and Killough, 1994; Campion *et al.*, 1996). OMRs have been popularly employed in many applications, especially in omni-directional wheelchairs (Wada and Asada, 1999), soccer player robots in RoboCup competitions (Samani *et al.*, 2004), and service robots (Qiu and Cao, 2008).

With the special mechanism of the omni-directional wheels, the driving torque required for each wheel is different while the robot moves along an arbitrary direction, this is called dynamic anisotropy in this paper. And the speed of each wheel is different while the robot moves along an arbitrary direction, this is called kinematic anisotropy. Especially, owing to the different applications (Tlale, 2006; Chatzakos *et al.*, 2006), the arrangement of the omni-directional wheels is not generally symmetrical, which makes the anisotropy much more distinct. Owing to the anisotropy of motion characteristics, the former motion control applicable for traditional mobile robots is not suitable for OMRs (Leng *et al.*, 2008). All of them considered the OMR as an isotropic problem and therefore the potential of OMRs were not fully exhibited.

Many motion control methods were proposed for OMRs in the past few years, but some of them only took into account the kinematics but not the dynamics. Daniel *et al.* (1985) presented the analytical model of the platform kinematics and described the results of preliminary open-loop control experiments. Wang *et al.* (2007) solved the time-optimal control problem as a constrained non-linear programming problem according to the kinematic model. Feng *et al.* (1989) described the design and implementation of a distributed servo-control system for the OMR which can execute

The current issue and full text archive of this journal is available at **www.emeraldinsight.com/0143-991X.htm**

Industrial Robot: An International Journal
37/1 (2010) 23–35

[DOI 10.1108/01439911011009939]

This paper is supported by the National High Technology Research and Development Program of China (863 Program), 2007AA041602-1.

Industrial Robot: An International Journal
Volume 37 · Number 1 · 2010 · 23–35

arbitrary trajectories specified by a sequence of three degrees-of-freedom (DOF) acceleration commands.

Most work on the control of OMR is based on the dynamic model and feedback method. Watanabe *et al.* (1998) developed the dynamic model of an OMR, and several control strategies are discussed based on linear control methods while the robot dynamics is non-linear (Watanabe, 1998). Purwin and D'Andrea (2006) took limited friction and vehicle dynamics into account, described an algorithm to calculate near-optimal minimum time trajectories for four wheeled omni-directional vehicles, which is based on a relaxed optimal control problem. Betourne and Campion (1996) devoted to the dynamic analysis of real redundant mobile robots, an output feedback linear control law is derived. Chen *et al.* (2002) presented an off-road omni-directional robot, which can run on an uneven road and obstacles, and also showed the adaptive control method for the OMR.

Although many work proposed the motion control based on the dynamics of OMR, the anisotropy is not introduced into the control system. Accordingly, the former motion control method cannot exhibit the potential of OMRs.

As a non-linear system for OMR, there are many uncertainties, such as slip (Williams *et al.*, 2002), non-linear rotational speed output from the DC motor, battery power fluctuations, etc. Owing to the non-linear and time-variance resulting from the above influential factors, it is difficult to deduce the exact control system model for the OMR. Therefore, it is necessary to find a robust control method for OMR. As a robust control method, sliding mode control (SMC) can overcome the influence of parametric vibrations and external disturbances. In the former research, it has been adopted in many robot control systems already, e.g. Yang and Kim (1999) proposed a robust tracking control of non-holonomic wheeled mobile robots using the sliding mode, and the proposed scheme is robust to bounded external disturbances.

It is well-known that SMC uses discontinuous control action to drive state trajectories toward a specific hyper-plane in the state space, and to maintain the state trajectories sliding on the specific hyper-plane until the origin of the state space is reached (Hung *et al.*, 1993; Hwang, 2002). This principle provides a guide to design a fuzzy controller for achieving system stability and satisfactory performance. Therefore, fuzzy sliding mode control (FSMC) combining two control principles can provide a robust controller for the non-linear systems (Hwang and Lin, 1992; Hwang and Chang, 2008), such as OMRs.

Motivated by the principle of the SMC, the control law often consists of equivalent control and switch control. The effect of equivalent control term is to force system state to slide on the sliding surface, and switch control is to derive the states toward the sliding surface. To improve the shortcomings such as the chattering phenomenon, a fuzzy controller is employed. Chen (1999) applied genetic algorithms to learning membership functions for obtaining an optimal fuzzy control, based on SMC, an expert fuzzy controller synthesized by a collection of fuzzy linguistic control rules is proposed. In Ha *et al.* (2001), FSMC is applied to the control of a hydraulically actuated mini-excavator.

The main objective of this work is to propose a motion control method for the OMR. According to the characteristics of OMR, we designed a fuzzy controller which is combined with SMC. In this control method, an influence factor k_s is introduced to the switch control to coordinate the driving torque. As a result, the control system is insensitive to parametric vibrations and external disturbances, and the chattering phenomenon is reduced.

With the special mechanism of omni-directional wheels, the different wheel arrangements, and the interaction force between the redundantly actuated wheels, it results in a dynamic anisotropy for OMRs. Based on the theory of vehicle dynamics, the acceleration and deceleration characteristic of each wheel is distinct. Therefore, when the robot moves along an arbitrary acceleration and direction, the driving torque acting on each wheel is different, and the rotational speed of each wheel is also different according to the kinematics. As a result, the slip phenomenon during the acceleration process is most prominent. Accordingly, it is important to pay more attention to this issue, but there is little research that deals with this problem for OMR in the past. To make each wheel achieve a coordinated motion, we translate the torque curve and rotational speed curve into an influential factor, which is also noted as anisotropy factor k_T. And the anisotropy factor is introduced to the switch control to coordinate the driving torque of each wheel output by FSMC. By introducing the anisotropy factor resulting from anisotropy, the robot can track the target speed precisely and quickly. Experiments were carried out and the results were promising. Finally, a new FSMC based on anisotropy is proposed in this paper.

2. Motion characteristics analysis

2.1 Kinematics modeling

There are many types of omni-directional wheels (Ferriere *et al.*, 1996). In this paper, we discuss the wheel which is shown in Figure 1. This omni-directional wheel assembly consists of a pair of "orthogonal wheels" (Pin and Killough, 1994). The wheel is composed of a driving roller and passive rollers, and the passive rollers are symmetrically distributed around the driving roller. It is obvious from Figure 1 that the axle ($\mathbf{S}_i$) of the driving roller intersects the axle ($\mathbf{E}_i$) of passive rollers, and the angle is 90°. The wheel is driven by the motor in a direction orthogonal to the wheel axle, and the passive rollers rotate in a direction parallel to the wheel axle. The OMR in Figure 2 uses these omni-directional wheels.

To design a robot with good performance, it is necessary to build the kinematic model for analyzing the velocity characteristics of the OMR (Angeles, 2003; Kalmár-Nagy *et al.*, 2004). According to the velocity relationship of the driving roller and the passive roller as shown in Figure 1, the velocity of the driving roller center o_i can be determined by:

$$\dot{o}_i = -R\dot{\theta}_i\mathbf{U}_i - r\dot{\phi}_i\mathbf{Z}_i \tag{1}$$

Meanwhile the velocity $\dot{o}_i$ also can be denoted by the velocity of robot center ($\dot{c}$) and angular velocity ω, and the equation is:

$$\dot{o}_i = \dot{c} + \omega\boldsymbol{\xi}\mathbf{d}_i \quad \text{where } \boldsymbol{\xi} \equiv \begin{bmatrix} 0 & -1 \\ 1 & 0 \end{bmatrix} \tag{2}$$

Owing to the passive rollers not being driven by a motor, the angular velocity of the passive roller $\dot{\phi}_i$ is irrelevant to our study, and can be eliminated during kinematic analysis. Dot-multiplied by the axle vector $\mathbf{E}_i$ on both sides of equations (1)

Figure 1 Omni-directional wheel

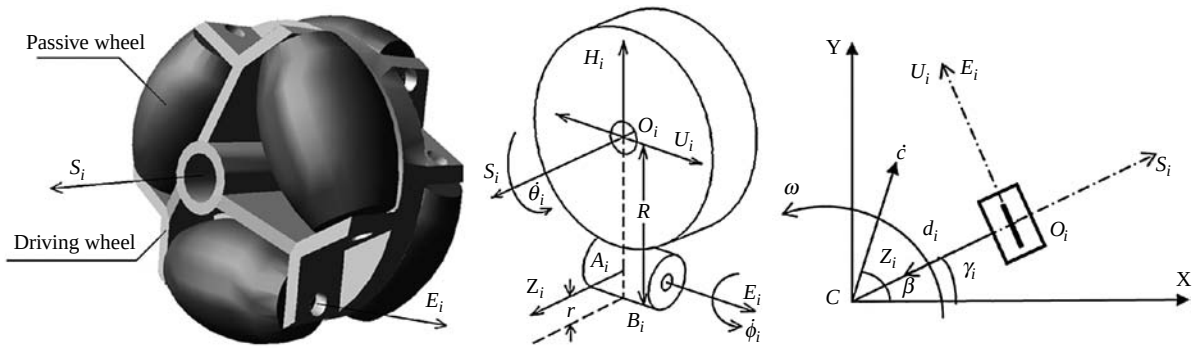

Figure 2 Omni-directional mobile robot

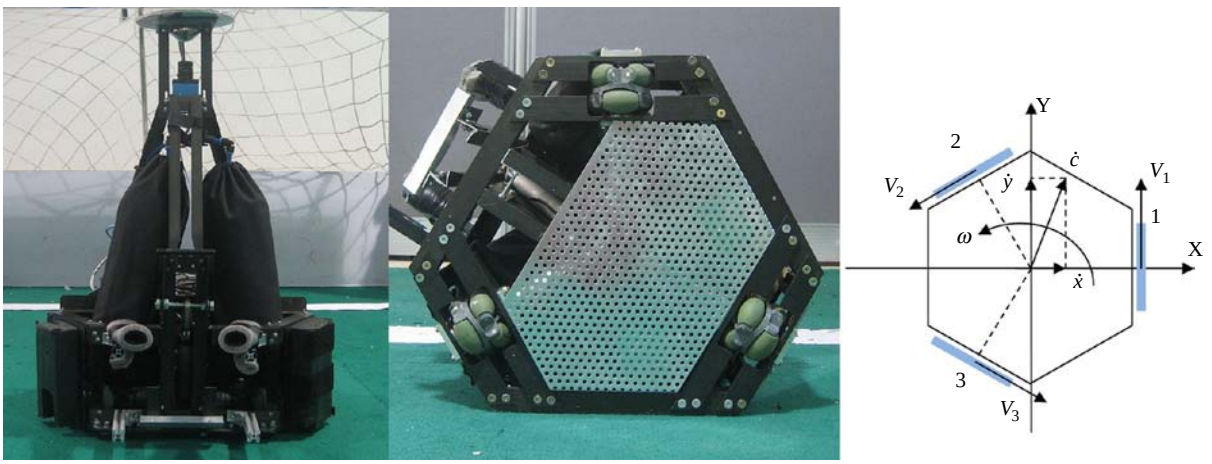

(a) (b) (c)

and (2), we can derive equation (3) as a general kinematic equation for the OMR:

$$-R\dot{\theta}_i = [\mathbf{E}_i \xi \mathbf{d}_i, \mathbf{E}_i]\mathbf{t}, \quad i = 1, 2, \ldots, n \quad \text{where } \mathbf{t} \equiv \begin{bmatrix} \omega \\ \dot{c} \end{bmatrix} \tag{3}$$

where:

- $\mathbf{d}_i$ — the vector from the point of robot center C to the point of driving roller center o_i;
- $\mathbf{d}_i = \mathrm{d}(i = 1, 2, \ldots, n)$, R and r — the radiuses of the driving roller and passive roller, respectively;
- $\dot{\theta}_i$ — the regular velocity of the driving roller; and
- $\mathbf{U}_i$ and $\mathbf{Z}_i$ — the vectors defined as in Figure 1.

According to the above analysis, the inverse kinematics equation of a three-wheeled OMR (Figure 2) can be deduced as:

$$\begin{pmatrix} \dot{\theta}_1 R \\ \dot{\theta}_2 R \\ \dot{\theta}_3 R \end{pmatrix} = \begin{pmatrix} 0 & 1 & d \\ -\sqrt{3}/2 & -1/2 & d \\ \sqrt{3}/2 & -1/2 & d \end{pmatrix} \begin{pmatrix} \dot{x} \\ \dot{y} \\ \omega \end{pmatrix} \tag{4}$$

And the forward kinematics equation is shown in equation (5):

$$\begin{pmatrix} \dot{x} \\ \dot{y} \\ \omega \end{pmatrix} = \begin{pmatrix} 0 & -\sqrt{3}/3 & \sqrt{3}/3 \\ 2/3 & -1/3 & -1/3 \\ 1/3d & 1/3d & 1/3d \end{pmatrix} \begin{pmatrix} \dot{\theta}_1 R \\ \dot{\theta}_2 R \\ \dot{\theta}_3 R \end{pmatrix} \tag{5}$$

The speed of each wheel is different while the robot moves along different directions, which is called as kinematic anisotropy. For example, the absolute speed value of each wheel is shown in Figure 3 while the linear speed is 1 m/s, and the angular speed is 0. The value β of the abscissa denotes the motion direction.

2.2 Dynamics modeling

The sum of the kinematic energy K of the robot is given in equation (6) (Viboonchaicheep *et al.*, 2003):

$$K = \frac{1}{2} \cdot m \cdot (\dot{x}^2 + \dot{y}^2) + \frac{1}{2} \cdot \mathcal{J}_\mathrm{r} \cdot \omega^2 + \frac{1}{2} \cdot \mathcal{J}_\mathrm{d} \cdot \left(\dot{\theta}_1^2 + \dot{\theta}_2^2 + \dot{\theta}_3^2\right) \tag{6}$$

where:

- m — the total mass of the robot;
- $\mathcal{J}_\mathrm{r}$ — the robot moment of inertia; and
- $\mathcal{J}_\mathrm{d}$ — the wheel's moment of inertia around the center of revolution.

Figure 3 Speed value curve of each wheel

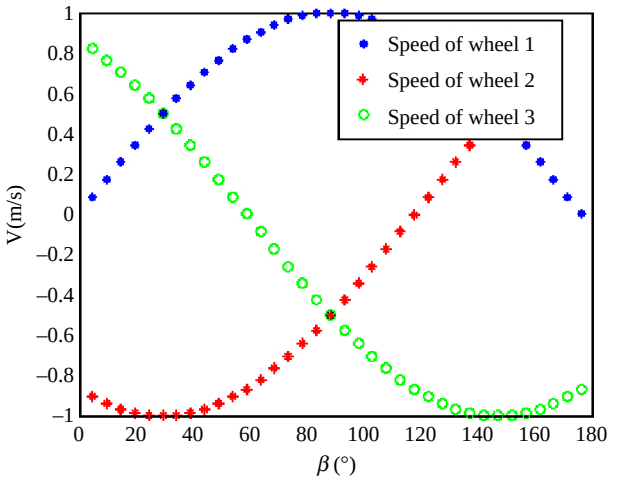

The loss energy is expressed as:

$$D = \frac{1}{2} \cdot D_\theta \cdot \left(\dot{\theta}_1^2 + \dot{\theta}_2^2 + \dot{\theta}_3^2 \right) \tag{7}$$

where:

D_θ the coefficient of the wheel's viscous friction.

Substituting equation (5) into (6) and utilizing Lagrangian equation:

$$\frac{\mathrm{d}}{\mathrm{d}t} \left(\frac{\partial K}{\partial \dot{\theta}_i} \right) - \frac{\partial K}{\partial \theta_i} = \tau_i \tag{8}$$

yields equation (9):

$$\tau = \mathbf{M}\ddot{\theta} + D_\theta \dot{\theta} \tag{9}$$

where:

$\dot{\theta} = [\,\dot{\theta}_1 \quad \dot{\theta}_2 \quad \dot{\theta}_3\,]^{\mathrm{T}}$ the rotational speed of each wheel; and
$\tau = [\,\tau_1 \quad \tau_2 \quad \tau_3\,]^{\mathrm{T}}$ the driving torque acting on each wheel.

$$\mathbf{M} = \begin{bmatrix} 2A + B + \mathcal{J}_\mathrm{d} & -A + B & -A + B \\ -A + B & 2A + B + \mathcal{J}_\mathrm{d} & -A + B \\ -A + B & -A + B & 2A + B + \mathcal{J}_\mathrm{d} \end{bmatrix}$$

$$\text{where } A = \frac{2mR^2}{9}, \quad B = \frac{\mathcal{J}_r R^2}{9d^2}$$

Based on the above equations, the state equation is yielded as:

$$\ddot{\mathbf{X}} = -\mathbf{N}\mathbf{M}^{-1} D_\theta \mathbf{N}^{-1} \dot{\mathbf{X}} + R\mathbf{N}\mathbf{M}^{-1}\tau + \mathbf{h} \tag{10}$$

where:

$$\dot{\mathbf{X}} = [\,\dot{x} \quad \dot{y} \quad \omega\,]^{\mathrm{T}}, \quad \mathbf{N} = \begin{pmatrix} 0 & -\sqrt{3}/3 & \sqrt{3}/3 \\ 2/3 & -1/3 & -1/3 \\ 1/3d & 1/3d & 1/3d \end{pmatrix}, \text{ and}$$

$\mathbf{h} = [\,h_1 \quad h_2 \quad h_3\,]^{\mathrm{T}}$ is the disturbance, $|h_i| < H$, H is the upper bound of disturbance.

3. Dynamic anisotropy analysis

3.1 Dynamics analysis

In other similar research, the wheels are assumed to be rigid bodies and non-deformable disks, and all interaction between the wheel and the ground is assumed to occur through a point contact. In reality, most wheels are made of a deformable material (such as rubber), so the interaction is through a contact patch and not a point.

Based on the theory of vehicle dynamics (Yu, 1990), while the OMR accelerates, the tangential force caused by the contact deformation between the driving wheel and the ground is the traction of the mobile robot. Rolling resistance couple resulting from the deformation of the wheel counteracts the rotation of the driving wheel, and the passive wheel is also subject to effects of the tangential force and resistance couple. The unitary force diagram and the force during the accelerating period of OMR are shown in Figure 4. And the parameters are defined in Table I.

According to the force diagram (Figure 4), the dynamic model of driving wheel and passive wheel (Yu, 1990) are defined by following equations:

$$m_\mathrm{d} a_{\mathrm{d}i} = f_{\mathrm{d}i} - F' \quad \mathcal{J}_\mathrm{d} \varepsilon_{\mathrm{d}i} = \tau_i - f_{\mathrm{d}i} R - M_{P_\mathrm{d}} \tag{11}$$

$$m_\mathrm{p} a_{\mathrm{p}i} = Q_\mathrm{p} - f_{\mathrm{p}i} \quad \mathcal{J}_\mathrm{p} \varepsilon_{\mathrm{p}i} = f_{\mathrm{p}i} r - M_{P_\mathrm{p}} \tag{12}$$

where:

m_d the mass of driving wheel; and
m_p the mass of passive wheel.

Figure 4 Force analysis

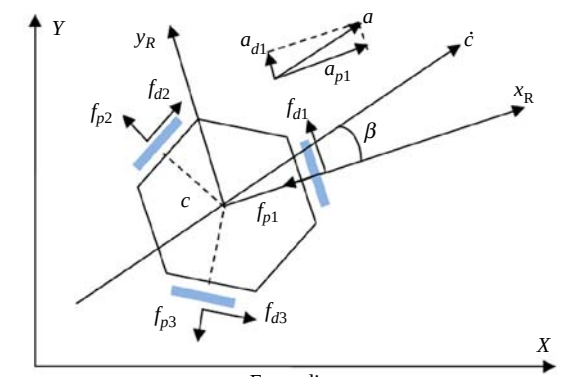

Table I Parameter definition

P_d, P_p	Gravitational loads acting on driving wheel and passive wheel
N_d, N_p	Normal counter-force acting on the driving wheel and passive wheel by the ground
f_{di}, f_{pi}	Tangential counter-force acting on the driving wheel and passive wheel by the ground at the point of contact
i	Sequence number of the wheel
F, Q_p	Component of forces acting on the driving wheel and passive wheel by the driving axis and passive axis
M_{P_d}, M_{P_p}	Rolling resistance moments acting on the driving wheel and passive wheel
ε_{di}, ε_{pi}	Angular accelerations of the driving wheel and passive wheel
a_{di}, a_{pi}	Components of acceleration of the driving wheel center and passive wheel center
J_d, J_p	Moments of inertia of the driving wheel and passive wheel
τ_i	Driving torque of the motor

3.2 Dynamic anisotropy

Owing to the special mechanism of omni-directional wheels and the existence of dynamic anisotropy, the driving torque acting on each wheel is distinct, when the robot moves in an arbitrary direction.

With inconsistent torque acting on the wheel, the rotational speed of the wheels cannot match each other. Then the robot cannot track the target speed during acceleration, and as a result, the slip phenomenon will be much more prominent during the acceleration than during other periods of motion. In order to avoid the uncoordinated motion between the three wheels, it is necessary to analyze the driving torque required by each wheel while the robot moves at an arbitrary speed and direction.

Owing to symmetry of the structure, only the case of $0 \le \beta \le 180°$ is discussed in this work. For simplification, it is assumed that the robot moves in direction β without rotation. To analyze the specifics of the driving torque, the driving torque acting on each wheel when the robot moves in different directions will be analyzed in the following section. In the following section, we will only analyze the case where the direction of acceleration β is subjected to $\beta < 30°$, and the force diagram is shown in detail in Figure 4(a).

As shown in Figure 4(a), in the local coordinate system $\{c, x_R, y_R\}$, suppose that the robot moves in the direction of β only with the translational motion, and the acceleration is a. Then according to the Newton's Second Law, we can obtain the following equations (13) and (14):

$$f_{d1} + f_{d3} = f_{d2} \tag{13}$$

$$\begin{aligned} &f_{d1}\sin(\beta) + f_{d2}\cos(\alpha-\beta) + f_{d3}\cos(\alpha+\beta) - f_{p1}\cos(\beta) \\ &\quad - f_{p2}\sin(\alpha-\beta) - f_{p3}\sin(\alpha+\beta) = ma \\ &f_{d1}\cos(\beta) + f_{d2}\sin(\alpha-\beta) - f_{d3}\sin(\alpha+\beta) + f_{p1}\sin(\beta) \\ &\quad + f_{p2}\cos(\alpha-\beta) - f_{p3}\cos(\alpha+\beta) = 0 \end{aligned} \tag{14}$$

where $\alpha = 30°$.

According to equation (12), the tangential counterforce acting on the passive wheel by the ground at the point of contact can be obtained by:

$$f_{pi} = \frac{\mathcal{J}_{pi} a_{pi}}{r^2} + \frac{M_{P_p}}{r}, \quad i = 1, 2, 3 \tag{15}$$

In Figure 4(a), the relation between a_{pi} and a is shown in equation (16):

$$\begin{aligned} a_{p1} &= a \cdot \cos(\beta) \\ a_{p2} &= a \cdot \cos(90 - \alpha + \beta) = a \cdot \sin(\alpha - \beta) \\ a_{p3} &= a \cdot \cos(90 - \alpha - \beta) = a \cdot \sin(\alpha + \beta) \end{aligned} \tag{16}$$

Substituting the equations (13)–(16) into equation (11), we can obtain the driving torque acting on driving wheel τ_i. With the same deduction, we can obtain τ_i while β varied in (0, 180°). In order to achieve intuitive cognition about the driving torque, we describe it in Figure 5. And the parameters needed for the computation are shown in Table II, where all of the values are determined according to the real robot.

4. Fuzzy sliding mode control

Owing to the uniqueness of an omni-directional wheel, the wheel moves in any direction with three DOF on a two-dimensional plane. And the interaction force between the redundantly actuated wheels results in slip phenomenon easily, which affects the motion control. As a non-linear component for DC motor, it is difficult to achieve multi-axis coordinated motion control. Also, because the power for DC motors is supplied by a portable battery, the non-linear characteristic of system is more apparent when the power decreases with respect to time during operation.

Owing to the above influential factors, the OMR exhibits non-linear and time-variant characteristics. It is difficult to build the exact mathematical model for the OMR motion controller. To find a more robust control for OMRs, first we propose a SMC method to overcome the uncertainty in

Figure 5 Driving torque acting on each wheel

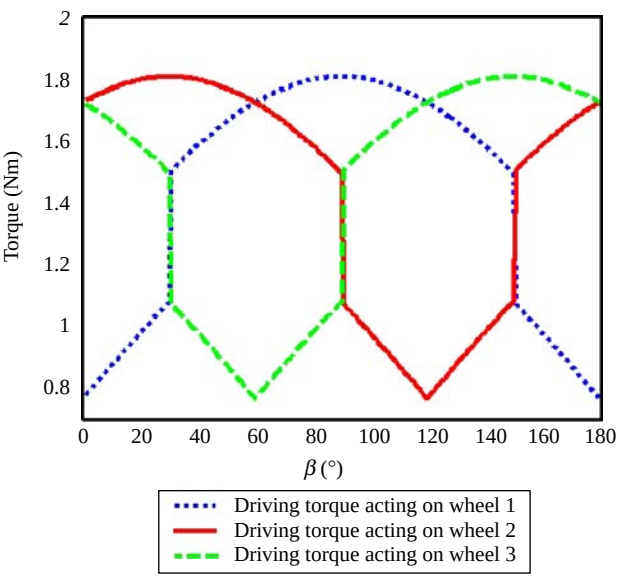

Table II Parameters for driving torque (SI units)

P (N)	R (mm)	r (mm)	a (m/s)^2	J_d (kg m^2)	M_{P_p} (N m)	M_{P_d} (N m)
196	0.2	0.04	1	0.011	0.392	0.147

this paper. But following this is the chattering phenomenon, which proves to be a considerable factor of interest for practical applications. In order to solve the problem, fuzzy control is introduced into the sliding mode controller here.

4.1 Sliding mode control

The robot is a typical non-linear system, and there are many unpredictable external disturbances. Owing to the characteristics of fast response and insensitive to parametric vibrations and disturbances, the SMC method is mainly applied to robot control in the recent years (Yu and Xu, 2000).

As in the commonly used SMC, the control law consists of equivalent control and switch control as:

$$\tau = \tau_{\text{eq}} + \tau_{\text{sw}} \tag{17}$$

The former is to force the system state to slide on the sliding surface, and the latter is to derive the states toward the sliding surface.

We define the sliding surface is $\mathbf{s} = \begin{bmatrix} s_1 & s_2 & s_3 \end{bmatrix} = \lambda^{\text{T}}\mathbf{E}$, where λ is the sliding surface coefficient vector. $\mathbf{E} = [e\dot{e}]^{\text{T}}$ is the error state vector, e is the tracking error. According to the effect of equivalent control, in sliding mode the equivalent control is described when the state trajectory is near $\mathbf{s} = 0$, and to yield an equivalent control law to keep state remaining on the sliding surface, it can be obtained by letting $\dot{s}$ equal zero.

For an OMR system, $\dot{s} = \lambda^{\text{T}}\dot{\mathbf{E}} + \ddot{\mathbf{X}}_d - \ddot{\mathbf{X}}$, where $\mathbf{X}_d$ is the target trajectory. Substituting the state equation (10) into it yields the equivalent control:

$$\tau_{\text{eq}} = \frac{(\mathbf{M}\mathbf{N}^{-1}(\lambda^{\text{T}}\dot{\mathbf{E}} + \ddot{\mathbf{X}}_d) + D_\theta\mathbf{N}^{-1}\dot{\mathbf{X}})}{R} \tag{18}$$

The purpose of switch control τ_{sw} is to guarantee the states move toward the sliding surface. Here, we define the switch control as:

$$\tau_{\text{sw}} = \frac{\mathbf{M}\mathbf{N}^{-1}\xi\,\text{sgn}(\mathbf{s})}{R} \tag{19}$$

where $\xi = [\,\xi_1 \quad \xi_2 \quad \xi_3\,]^{\text{T}}$, $\xi_i > 0$, $\text{sgn}(\cdot)$ is the Sign function.

Substituting the above equations into $\dot{\mathbf{s}} = \lambda^{\text{T}}\ddot{\mathbf{E}} + \dddot{\mathbf{X}}_d - \dddot{\mathbf{X}}$, we can obtain:

$$s_i\dot{s}_i = s_i \cdot (-\xi_i \cdot \text{sgn}(s_i)) - s_i \cdot h_i = -\xi_i|s_i| - s_i h_i \tag{20}$$

To guarantee the control system is stabilized, a Lyapunov function candidate is given as:

$$V = \frac{1}{2}s_i^2 \tag{21}$$

Then differentiate V with respect to time. Based on the stability of SMC condition, we have:

$$\dot{V} = s_i\dot{s}_i < 0 \tag{22}$$

According to the above analysis, we can achieve a stable SMC system when $\xi_i \geq \text{RH}$.

4.2 Fuzzy sliding mode controller

To reduce susceptibility to parametric vibrations and external disturbances, the control output is operating or chattering at a high frequency. The chattering may result in a bad influence on motors and other equipments of the servo system. And the tracking error may be chattering near zero point, accordingly to increase the steady-state error. As a result of chattering, parasitic oscillation will occur, finally the control system performance will be influenced (Ha *et al.*, 2001). To reduce the chattering phenomenon in the sliding mode, fuzzy tuning schemes are employed in this paper. A coordinating parameter k_s is introduced into the traditional SMC to reduce the chattering phenomenon. We define the control law as:

$$\tau = \tau_{\text{eq}} + k_s \cdot \tau_{\text{sw}} \tag{23}$$

For the stability of control system, as analyzed in Section 4.1, $k_s\xi_i \geq \text{RH}$ must be guaranteed.

When the rotational speed of any wheel is close to the target speed, it is better to reduce the value k_s to reduce the speed while crossing the sliding mode surface. And it is better to keep a big value k_s to ensure high velocity, when the rotational speed has not reached the target speed. Therefore, taking the tracking error of speed for each wheel e_{wi} as input, and taking the coordinating parameter k_s as output, we design the fuzzy sliding mode controller. The robot system consists of three wheels, so there are three independent fuzzy controllers. In the following section, we will describe the design of the fuzzy controller.

Defining the universe of discourse for input variable as e_{wi} for each wheel fuzzy controller in $[-a_1,a_1]$, and the universe of discourse for output variable k_s in $[0,b_4]$, where a_i and b_i are noted in Figures 6 and 7, $i = 1, 2, 3, 4$. The fuzzy subset of linguistic value for input and output variables is set as {PB, PM, PS, ZO, NB, NM, NS}.

The design principle for the fuzzy controller rule is described as follows. As a fundamental requirement, the target reach and rapidity must be guaranteed. Accordingly, when the rotational speed is far away from target speed, the amplitude of switch control term should be big, whereas it should be reduced when the rotate speed is close to target speed. According to the conventional fuzzy condition and fuzzy relation, we consider the following fuzzy control rules:

Figure 6 The membership function of input

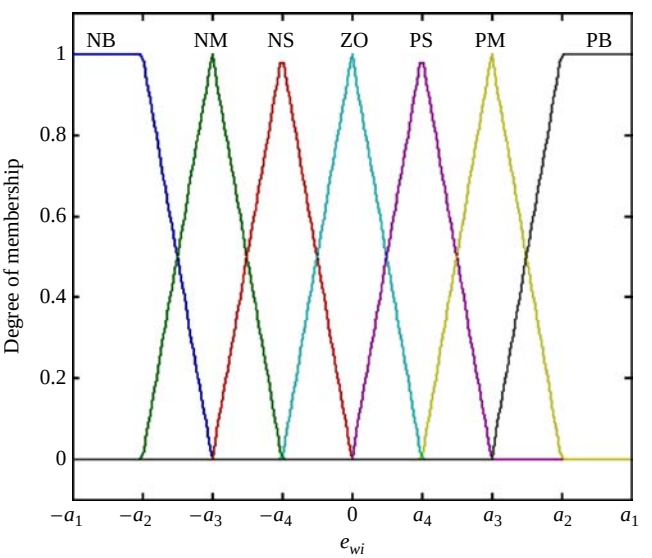

Figure 7 The membership function of output

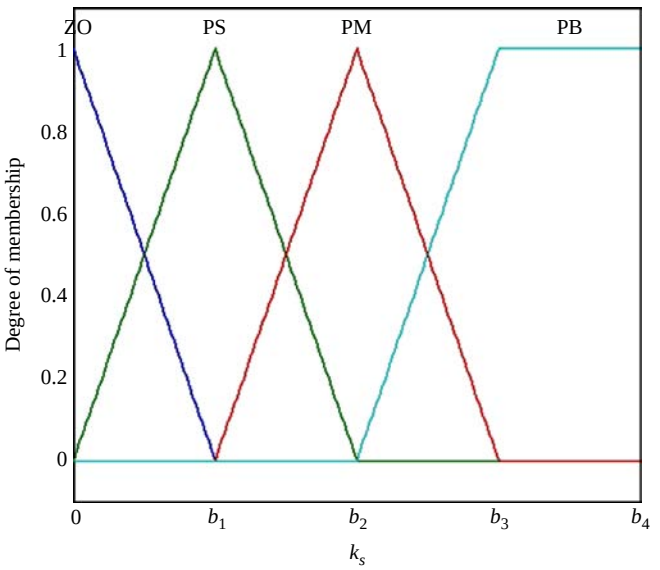

$$R_i: \quad \text{If } e_{wi} \text{ is } A_i, \quad \text{then } k_s \text{ is } B_i$$

where:

R_i denotes the ith rule;
A_i the ith fuzzy set; and
B_i the ith output.

The fuzzy control rules are shown in Table III.

Without loss of generality, the membership functions of fuzzy sets are all considered as triangle typed and shown in Figures 6 and 7 for input and output, respectively. Obviously, the definition of adjoining membership functions are overlap and symmetrical. And we employ the centroid method as a de-fuzzification method to transform the fuzzy output into exact output in this paper.

4.3 Simulation results

In order to validate the feasibility of application to OMR system for FSMC, we conducted simulation comparisons for the effectiveness between fuzzy SMC and traditional SMC. The simulation is realized by Matlab/Simulink. The simulation object is the three-wheeled OMR shown in Figure 2. To be as close to the practical effect as possible, the parameters used in the simulation are determined according to the real robot. The main part of the initial setup for the simulation is shown in Table IV, other parameters are shown in Table II.

The control block diagram is shown in Figure 8. To emulate the real case, we introduce the Gaussian Function disturbance into the system state equation, which is defined as:

$$h_i(t) = A \cdot \exp\left(-\frac{(t-c)^2}{2b^2}\right) \tag{24}$$

where $A = 8$, $b = 0.5$, $c = 3$. And the upper bound of disturbance is defined as $H = \max(|h(t)|) + \eta$, where $\eta = 1$.

In the simulation, we compare the chattering phenomena resulting from the fuzzy SMC and traditional SMC, by tracking a circular trajectory, also the anti-disturbance ability and the trajectory tracking effect is presented. The circular trajectory is defined as:

$$\begin{cases} x_d = \cos t \\ y_d = \sin t \\ \phi_d = t \end{cases} \tag{25}$$

As shown in Figure 9, the traditional SMC also can eliminate the disturbance influence, and it can achieve good tracking results. But the control output appears with significant chattering phenomenon, which will result in bad influence for the real robot system, while there is almost no chattering phenomenon for the SMC combined with fuzzy control. According to the comparison, it has proven the advantage for the FSMC weakening the chattering phenomenon.

5. FSMC based on anisotropy

5.1 Control method

The interaction force between wheel and ground is not taken into account for the dynamics model used in the control system above. It leads to difficulty of exhibiting the real response of each wheel in the real robot motion. Therefore, there are some limits in the practical robot control with the control method above.

Owing to the special mechanism of omni-directional wheels and the different wheel arrangement, the dynamic anisotropy is distinct for OMRs. The force acting on each wheel is different while the robot moving in different direction, i.e. the driving torque acting on each wheel is different. Influenced by the frictional force, which results from the contact between the wheel and the ground, it also leads to the dynamic anisotropy. With the guarantee that the fuzzy SMC is stable, by introducing the influence factor of dynamic anisotropy into the control system, the driving torque acting on each wheel is coordinated while the robot moves in different direction. As a result, it can achieve a

Table III Rule for FSMC

e_{wi}	PB	PM	PS	ZO	NB	NM	NS
k	PB	PM	PS	ZO	PB	PM	PS

Table IV Setup for simulation (SI units)

J_r (kg m^2)	J_p (kg m^2)	$\|d_i\|$ (m)	D_θ	a_1	a_2	a_3	a_4	b_1	b_2	b_3	b_4	ξ_i
0.3562	0.5482×10^{-4}	0.22	0.3	10	4	1	0.5	0.2	0.6	1	1.5	13

Figure 8 Control system block diagram

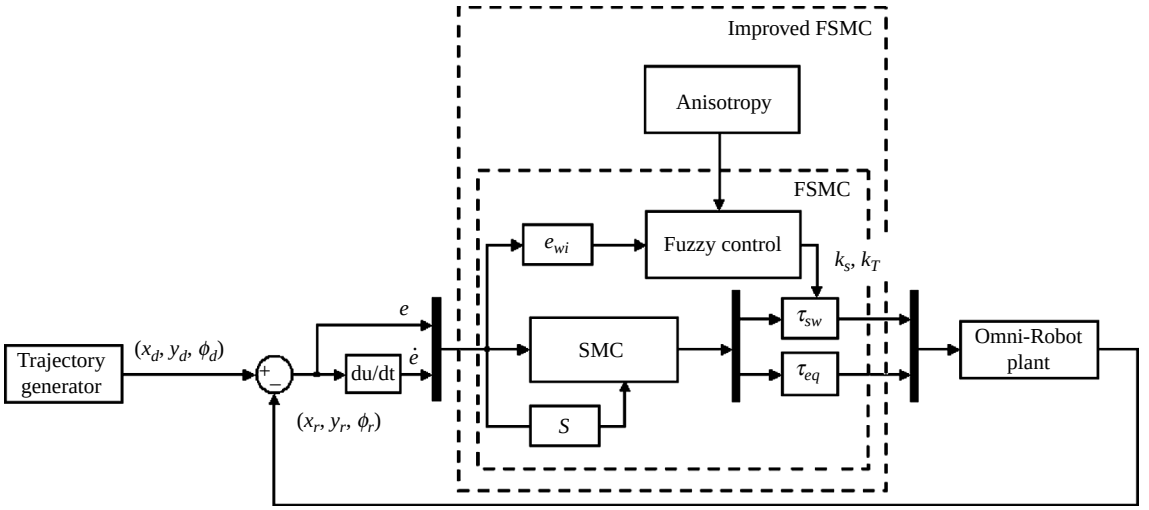

good speed and trajectory tracking with rapidity and accuracy, also the slip phenomenon can be reduced to some extent.

In order to ensure that the robot moves along the target direction throughout the motion process, whether during the acceleration process or during the process of uniform motion, the rotational speed of wheels should be coordinated with each other, or else the robot will not move in the specified target direction. While the robot moves only with the translation, there will be some form of rotational motion occurring without coordinated motion control, especially when it has not reached steady state motion. Therefore, the target rotational speed and the force condition of each wheel must be taken into consideration during the motion control.

According to the analysis above about the driving torque acting on different wheels while the robot moves in different directions, the following conclusion can be deduced. When the driving torque needed for any wheel is big, the corresponding k_T should be big, vice versa. And for a faster target speed, the higher the acceleration should be, i.e. the corresponding driving torque should be higher or vice versa. Accordingly, the speed and driving torque characteristics of each wheel are processed as the influential factor together.

For the three-wheeled OMR discussed in this paper, according to the analysis on the kinematics in the above section, we can obtain the absolute speed value of each wheel, while it moves in the speed of 1 m/s in some arbitrary direction. Owing to the symmetry, only the case of 0-180° is presented here.

First of all, we obtain the absolute value of speed (Figure 3), and convert both the value of speed and driving torque (Figure 5) into [0, 1], which are denoted by $V(\beta)$ and $T(\beta)$, respectively. And then, the influential factor k_T, which is also known as the anisotropy factor, is defined as:

$$k_T = n_v V(\beta) + n_T T(\beta) \tag{26}$$

where:

n_v and n_T the influential weights of speed and driving torque, respectively.

For example, when both of them are defined as 50 percent, then the influential factor curve is shown in Figure 10.

Taking into consideration, the anisotropy characteristics and the contact interaction force, we introduce the influential factor k_T into the control system. The control law is defined as:

$$\tau = \tau_{\text{eq}} + (k_s + k_T)\tau_{\text{sw}} \tag{27}$$

To ensure that the system introduced by anisotropy factor is stable, according to the analysis in Section 4.1, we should also ensure that $(k_s + k_T)\xi_i \geq \text{RH}$.

5.2 Experiment results

In order to verify the effectiveness of the FSMC based on anisotropy, we carried out some experiments on the real robot. The experiment results using improved FSMC method are compared with the results using traditional FSMC method. Line trajectory and circular trajectory tracking motions are discussed in the experiments.

In the experiments, the omni-directional middle-size soccer robot (Figure 2) is used, and the omni-directional wheels are all side rollers (diameter 80 mm). The weight of the robot is about 20 kg, and the dimensions are $45 \times 45 \times 80$ mm.

The experiment is carried out on the green-carpeted field for RoboCup middle-sized robots (12×8 m, with reference to the RoboCup rules before 2007).

We carried out some experiments with different influential weights, then chose the experimental result with best effectiveness of control and determined the corresponding influential weights as the final values. Here, the values are $n_v = 0.4$ and $n_T = 0.6$.

When the robot is moving during the acceleration process, due to the existing anisotropy of each wheel, it is difficult to achieve coordinated motion. To exhibit the motion error resulting from the non-synchronous motion during the acceleration process, we set the rotational speed at 0, i.e. there is only translation.

For the line trajectory tracking motion, we let the robot move at 1 m/s along a 45° direction, and speed of each wheel is shown in Figure 11(a) and (b). Though the rotational speed is set at 0, according to Figure 11(c) and (d), we can see that high angular speed occurs during the acceleration process. It results in the motion direction deviating from the target

Figure 9 Simulation result comparisons

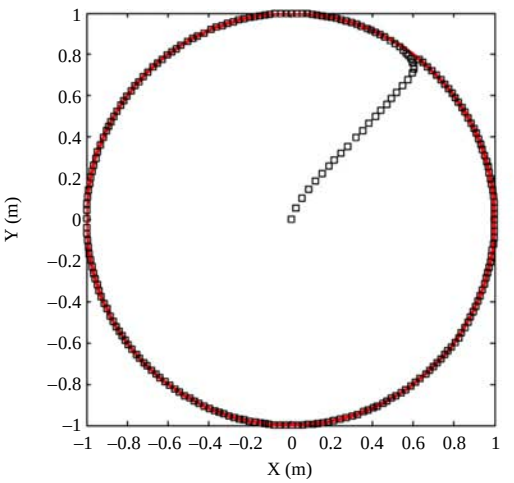

(a) Trajectory result using SMC

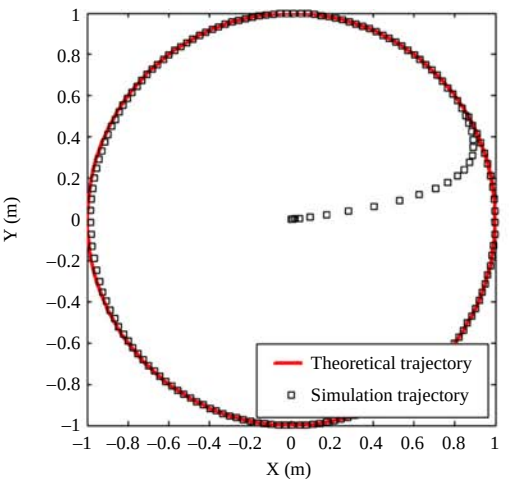

(b) Trajectory result using FSMC

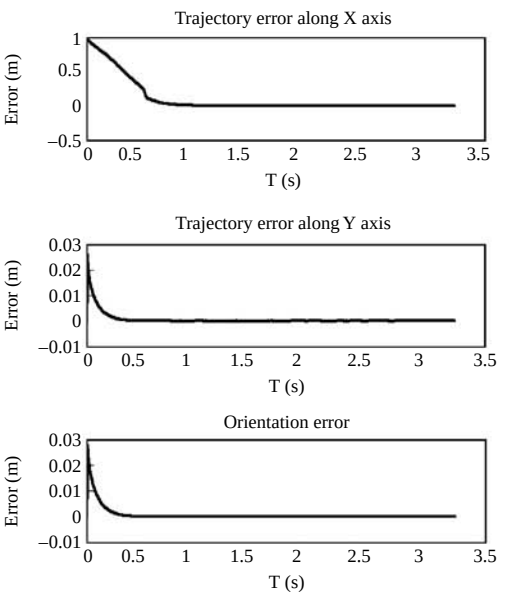

(c) Trajectory error using SMC

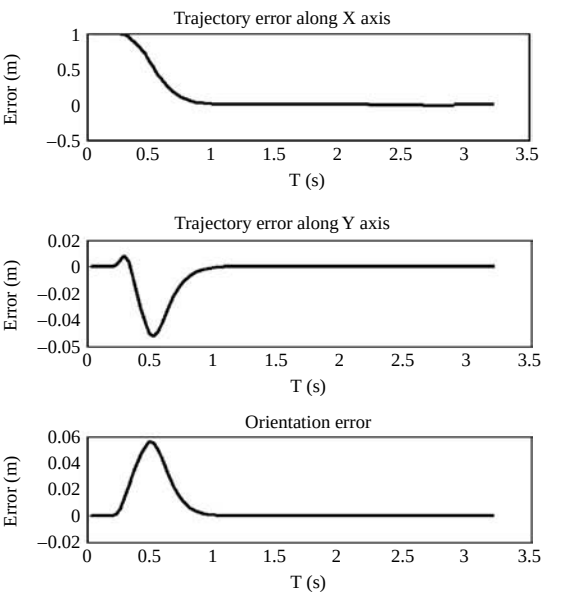

(d) Trajectory error using FSMC

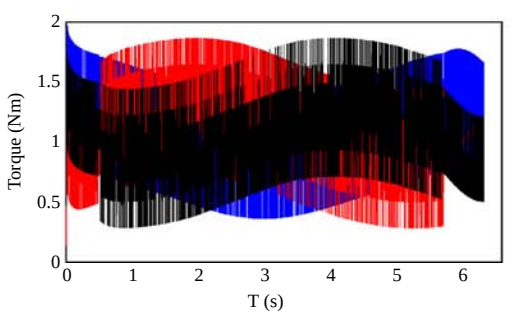

(e) Driving torque curve using SMC

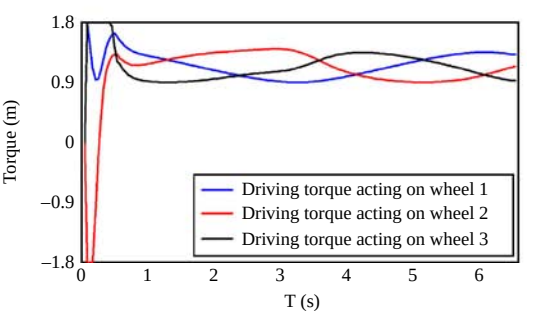

(f) Driving torque curve using FSMC

Figure 10 Anisotropy factor

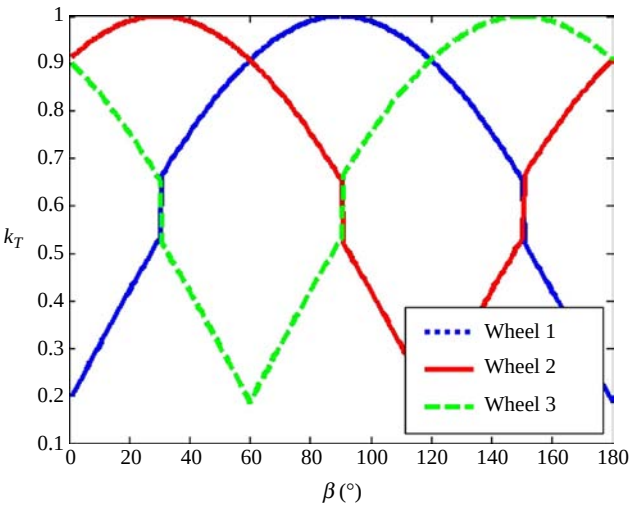

direction when the robot speeds up to the target speed as shown in Figure 11(e). In the case of no sensors installed onto the robot such as a vision sensor, the robot will move in the wrong direction. In the experiments, we only use encoder data for control feedback. The trajectories of the experiment results are calculated from the encoder data of each wheel. From Figure 11(g) to (h), we can find out that after speeding up to the target speed, the robot can move along a line, and the rotational speed error is constrained to a limited range.

For the circular trajectory tracking motion, we let the robot move at 1.1 m/s, and the radius of the circular trajectory is 2 m. During the motion the rotational speed of each wheel (Figure 12(a) and (b)) is changing with respect to time. From Figure 12(c) to (d), it is clear that angular speed errors occur, especially during the acceleration process. According to tracking results in Figure 12(e)-(h), the trajectory error is distinct especially with the FSMC method not based on the anisotropy.

Comparing the experimental results using traditional FSMC and FSMC based on anisotropy, we can conclude that both the line trajectory tracking and circular trajectory tracking, the tracking error of the latter method is smaller than the former one. For example, in line trajectory tracking motion with traditional FSMC method, the rotational speed error is significant during the acceleration process, while it is smaller with the improved FSMC, comparing with (c) and (d) of Figure 11. Owing to the speed variation in all motion processes for circular trajectory tracking motion, the large rotational speed error exists throughout for traditional FSMC, while it is not the case for the improved FSMC, comparing with (c) and (d) of Figure 12.

From the line trajectory and circular trajectory tracking motion experiment results, when the rotational speed of the wheel is changing or accelerating, the wheels cannot achieve coordinated motion, and a large angular speed error occurs. For example, in the line trajectory tracking motion, the target speed of wheel 2 is higher than the other two, and the driving torque required is the largest. Accordingly, wheel 2 accelerates slowly with traditional motion control, and it cannot achieve synchronous motion with the other two wheels. After introducing the anisotropy factor, the angular speed error resulted from the non-synchronous motion is distinctly reduced.

In the line trajectory tracking motion experiments, although the ground is uneven, the robot control system is insensitive to parametric vibrations and external disturbances. When the robot sped up to the target speed and moves at a constant speed, the robot can overcome the influence of non-linear characteristics, and the angular speed error is constrained to a limited range. According to the experiment results above, we can conclude that by introducing the anisotropy factor into the FSMC method, it can achieve invariant control and a coordinated motion quickly.

6. Conclusion

Different from traditional mobile robot, it is difficult to achieve a coordinated motion for the multi-axis system of OMRs during the acceleration process with the existence of anisotropy, so as not to be able to achieve exact translational motion along some directions. Taking into consideration, the friction and other interactive forces between the wheel and ground, we analyzed the relation between driving torques acting on each wheel, and proposed a novel concept of dynamic anisotropy for OMRs in this paper. We introduced an anisotropy factor into FSMC method based on the anisotropy. Then a new FSMC method is proposed in this paper. By coordinating the driving torque with the anisotropy factor, each wheel can speed up to the target speed, and the resulting motion trajectory is greatly improved. With the proposed control method, the robot control system is insensitive to parametric vibrations and external disturbances, and the chattering phenomenon is reduced. Simulations and experiments have proven that each wheel can achieve a coordinated motion, and an effective motion tracking can be achieved by using the proposed motion control method.

In order to obtain a clearer analysis of the anisotropy influence during the acceleration process, only the translation motion case is discussed in this paper. The case with both translation and rotation motion will be dealt with in future research.

Figure 11 Experimental data of line tracking motion

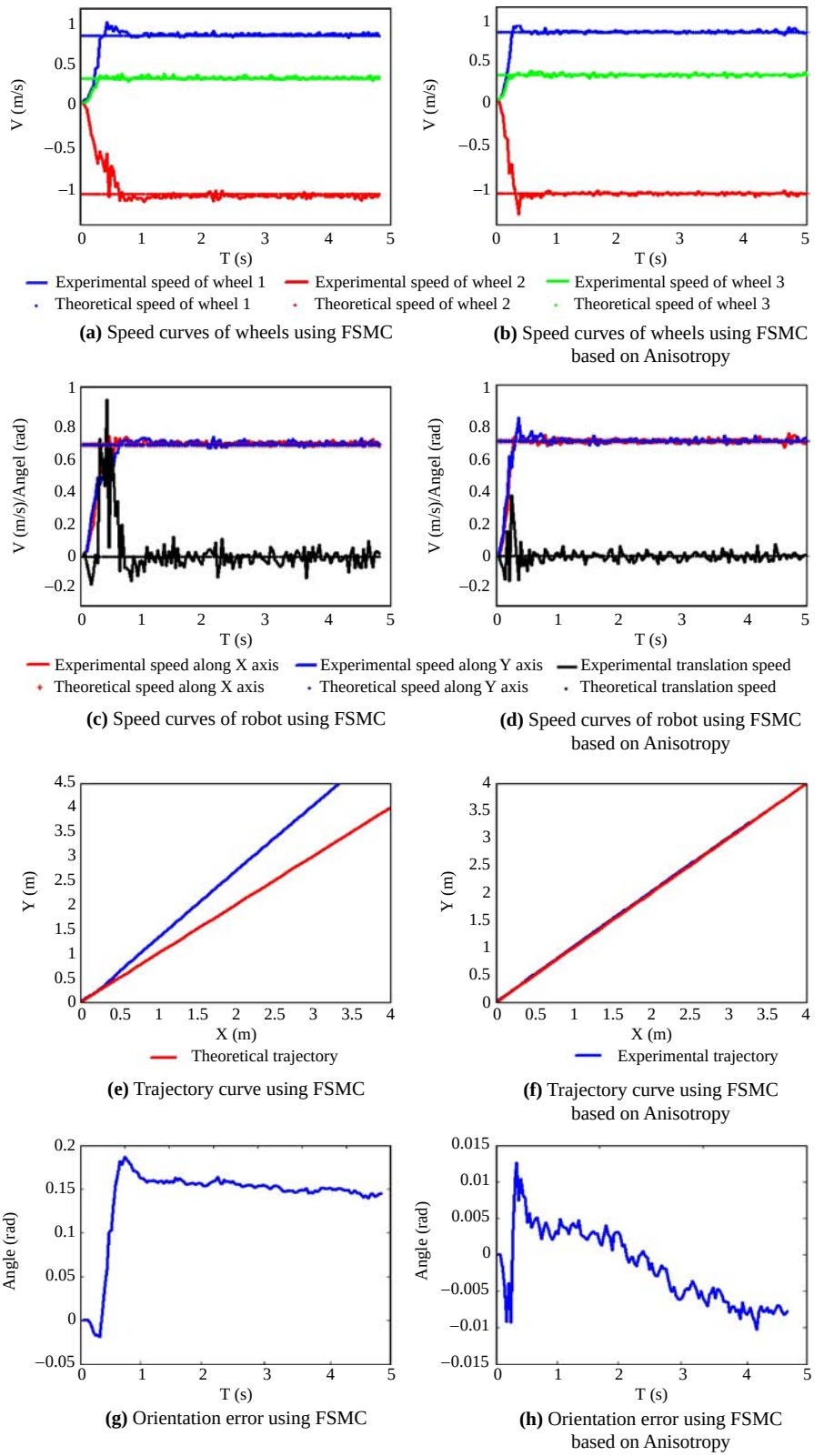

(a) Speed curves of wheels using FSMC

(b) Speed curves of wheels using FSMC based on Anisotropy

(c) Speed curves of robot using FSMC

(d) Speed curves of robot using FSMC based on Anisotropy

(e) Trajectory curve using FSMC

(f) Trajectory curve using FSMC based on Anisotropy

(g) Orientation error using FSMC

(h) Orientation error using FSMC based on Anisotropy

Figure 12 Experimental data of circular trajectory tracking motion

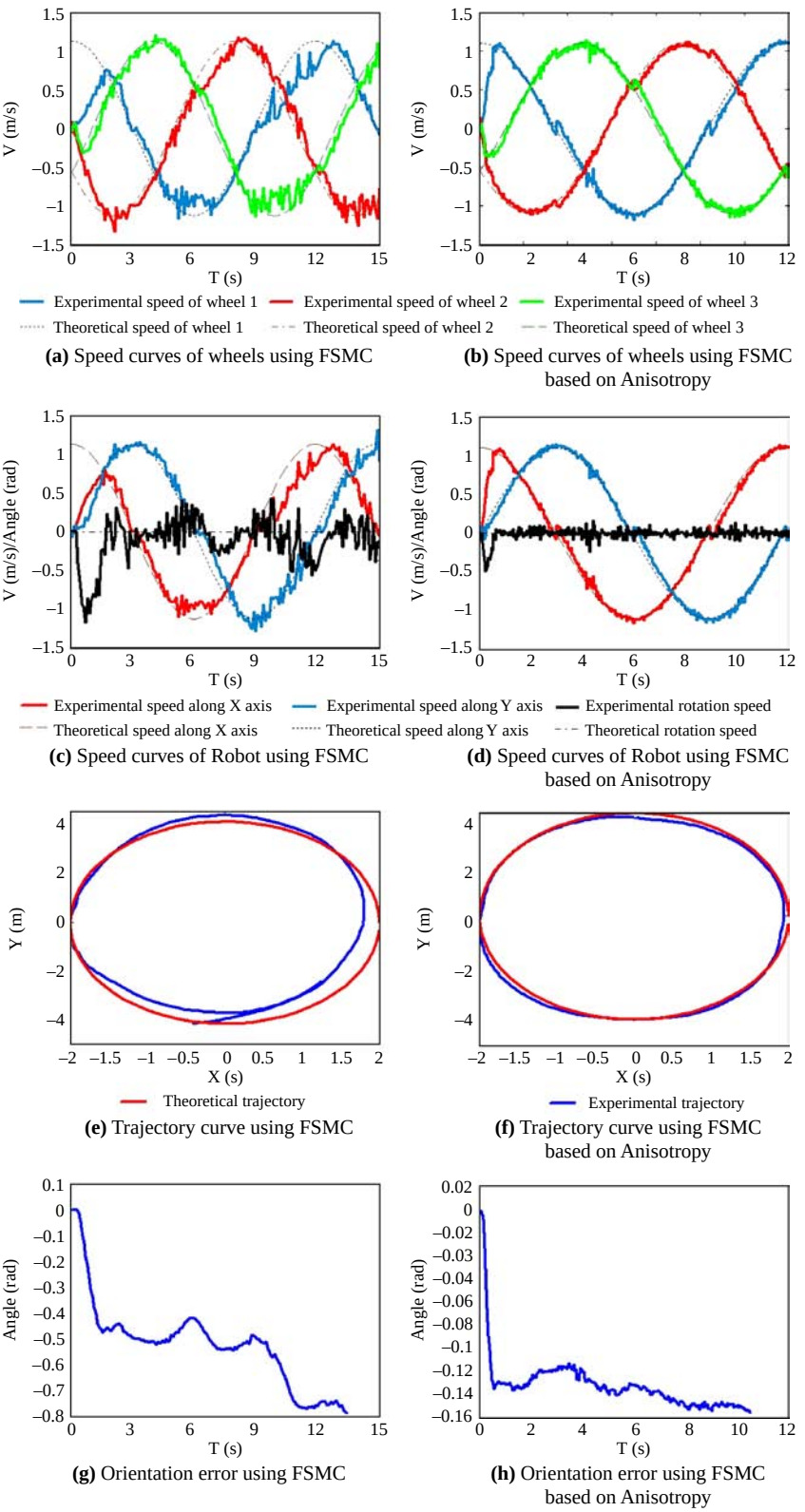

(a) Speed curves of wheels using FSMC

(b) Speed curves of wheels using FSMC based on Anisotropy

(c) Speed curves of Robot using FSMC

(d) Speed curves of Robot using FSMC based on Anisotropy

(e) Trajectory curve using FSMC

(f) Trajectory curve using FSMC based on Anisotropy

(g) Orientation error using FSMC

(h) Orientation error using FSMC based on Anisotropy

References

Angeles, J. (2003), *Fundamentals of Robotic Mechanical Systems: Theory, Methods, and Algorithms*, 2nd ed., Springer, New York, NY.

Betourne, A. and Campion, G. (1996), "Dynamic modeling and control design of a class of omnidirectional mobile robots", *IEEE International Conference on Robotics and Automation, Minneapolis, MN*, pp. 2810-15.

Campion, G., Bastin, G. and D'Andrea Novel, B. (1996), "Structural properties and classification of kinematic and dynamic models of wheeled mobile robots", *IEEE Transactions on Robotics and Automation*, Vol. 12 No. 1, pp. 47-62.

Chatzakos, P., Markopoulos, Y.P., Hrissagis, K. and Khalid, A. (2006), "On the development of a modular external-pipe crawling omni-directional mobile robot", *Industrial Robot: An International Journal*, Vol. 33 No. 4, pp. 291-7.

Chen, J.Y. (1999), "Expert SMC-based fuzzy control with genetic algorithms", *Journal of The Franklin Institute*, Vol. 336 No. 4, pp. 589-610.

Chen, P., Mitsutake, S., Isoda, T. and Shi, T. (2002), "Omni-directional robot and adaptive control method for off-road running", *IEEE Transactions on Robotics and Automation*, Vol. 18 No. 2, pp. 251-6.

Daniel, D., Krogh, B. and Friedman, M. (1985), "Kinematics and open-loop control of an ilonator-based mobile platform", *Proceedings of the 1985 IEEE International Conference on Robotics and Automation (ICRA'85)*, pp. 346-51.

Feng, D., Friedman, M.B. and Krogh, B.H. (1989), "The servo-control system for an omnidirectional mobile robot", *IEEE International Conference on Robotics and Automation*, Vol. 3, pp. 1566-71.

Ferriere, L., Raucent, B. and Campion, G. (1996), "Design of omnimobile robot wheels", *Proceedings of the IEEE International Conference on Robotics and Automation, Minneapolis, MN, USA*, pp. 3664-70.

Ha, Q.P., Nguyen, Q.H., Rye, D.C. and Durrant-Whyte, H.F. (2001), "Fuzzy sliding-mode controllers with applications", *IEEE Transactions on Industrial Electronics*, Vol. 48 No. 1, pp. 38-46.

Hung, Y., Gao, W. and Hung, J.C. (1993), "Variable structure control: a survey", *IEEE Transactions on Industrial Electronics*, Vol. 40 No. 1, pp. 2-22.

Hwang, C.L. (2002), "Robust discrete variable structure control with finitetime approach to switching surface", *Automatica*, Vol. 38 No. 1, pp. 167-75.

Hwang, C.L. and Chang, N.W. (2008), "Fuzzy decentralized sliding-mode control of a car-like mobile robot in distributed sensor-network spaces", *IEEE Transactions on Fuzzy Systems*, Vol. 16 No. 1, pp. 97-109.

Hwang, G.C. and Lin, S.C. (1992), "A stability approach to fuzzy control design for nonlinear systems", *Fuzzy Sets and Systems*, Vol. 48 No. 3, pp. 279-87.

Kalmár-Nagy, T., D'Andrea, R. and Ganguly, P. (2004), "Near-optimal dynamic trajectory generation and control of an omnidirectional vehicle", *Robotics and Autonomous Systems*, Vol. 46 No. 1, pp. 47-64.

Leng, C.T., Cao, Q.X. and Huang, Y.W. (2008), "A motion planning method for omni-directional mobile robot based on the anisotropic characteristics", *International Journal of Advanced Robotic Systems*, Vol. 5 No. 4, pp. 327-40.

Pin, F.G. and Killough, S.M. (1994), "A new family of omni-directional and holonomic wheeled platforms for mobile robots", *IEEE Transactions on Robotics and Automation*, Vol. 10 No. 4, pp. 480-9.

Purwin, O. and D'Andrea, R. (2006), "Trajectory generation and control for four wheeled omnidirectional vehicles", *Robotics and Autonomous Systems*, Vol. 54 No. 1, pp. 13-22.

Qiu, C.W. and Cao, Q.X. (2008), "Modeling and analysis of the dynamics of an omni-directional mobile manipulators system", *Journal of Intelligent and Robotic Systems: Theory and Applications*, Vol. 52 No. 1, pp. 101-20.

Samani, A.H., Abdollahi, A., Ostadi, H. and Rad, S.Z. (2004), "Design and development of a comprehensive omni-directional soccer player robot", *International Journal of Advanced Robotic Systems*, Vol. 1 No. 3, pp. 191-200.

Tlale, N.S. (2006), "On distributed mechatronics controller for omni-directional autonomous guided vehicles", *Industrial Robot: An International Journal*, Vol. 33 No. 4, pp. 278-84.

Viboonchaicheep, P., Shimada, A. and Kosaka, Y. (2003), "Position rectification control for Mecanum wheeled omni-directional vehicles", *The 29th Annual Conference of the IEEE Industrial Electronics Society*, Vol. 1, pp. 854-9.

Wada, M. and Asada, H.H. (1999), "Design and control of a variable footprint mechanism for holonomic omnidirectional vehicles and its application to wheelchairs", *IEEE Transactions on Robotics and Automation*, Vol. 15 No. 6, pp. 978-89.

Wang, S.M., Lai, L.C., Wu, C.J. and Shiue, Y.L. (2007), "Kinematic control of omni-directional robots for time-optimal movement between two configurations", *Journal of Intelligent and Robotic Systems*, Vol. 49 No. 4, pp. 397-410.

Watanabe, K. (1998), "Control of an omnidirectional mobile robot", *Proceedings of the 2nd International Conference on Knowledge-based Intelligent Electronic Systems*, pp. 51-60.

Watanabe, K., Shiraishi, Y. and Tzaffestas, S.G. (1998), "Feedback control of an omnidirectional autonomous platform for mobile serve robots", *Journal of Intelligent and Robotic Systems*, Vol. 22 No. 3, pp. 315-30.

Williams, R.L., Carer, B.E., Gallina, P. and Rosati, G. (2002), "Dynamic model with slip for wheeled omnidirectional robots", *IEEE Transactions on Robotics and Automation*, Vol. 18 No. 3, pp. 285-93.

Yang, J.M. and Kim, J.H. (1999), "Sliding mode control for trajectory tracking of nonholonomic wheeled mobile robots", *IEEE Transactions on Robotics and Automation*, Vol. 15 No. 3, pp. 578-87.

Yu, X.H. and Xu, J.X. (2000), *Advances in Variable Structure Systems*, World Scientific, Singapore.

Yu, Z.S. (1990), *Automoblie Theory*, China Machine, Beijing.

Corresponding author

Chuntao Leng can be contacted at: ctleng@sjtu.edu.cn